



## RESEARCH LETTER

10.1029/2023GL103045

## Earthquake Magnitude With DAS: A Transferable Data-Based Scaling Relation

Jiuxun Yin<sup>1</sup> , Weiqiang Zhu<sup>1</sup>, Jiaxuan Li<sup>1</sup>, Ettore Biondi<sup>1</sup> , Yaolin Miao<sup>2</sup>, Zack J. Spica<sup>2</sup> , Loïc Viens<sup>3</sup> , Masanao Shinohara<sup>4</sup> , Satoshi Ide<sup>5</sup> , Kimihiro Mochizuki<sup>4</sup> , Allen L. Husker<sup>1</sup> , and Zhongwen Zhan<sup>1</sup>

## Key Points:

- We present the first data-based scaling relation between Distributed Acoustic Sensing (DAS) amplitude and earthquake magnitude
- Earthquake magnitude can be reliably estimated from DAS amplitude with the scaling relation
- The DAS scaling relation can be transferred from one region to another with minor calibrations

## Supporting Information:

Supporting Information may be found in the online version of this article.

## Correspondence to:

J. Yin,  
yinjx@caltech.edu

## Citation:

Yin, J., Zhu, W., Li, J., Biondi, E., Miao, Y., Spica, Z. J., et al. (2023). Earthquake magnitude with DAS: A transferable data-based scaling relation. *Geophysical Research Letters*, 50, e2023GL103045. <https://doi.org/10.1029/2023GL103045>

Received 31 JAN 2023

Accepted 7 MAY 2023

## Author Contributions:

**Conceptualization:** Jiuxun Yin

**Data curation:** Jiuxun Yin, Weiqiang Zhu, Jiaxuan Li, Ettore Biondi, Yaolin Miao, Masanao Shinohara

**Formal analysis:** Jiuxun Yin

**Funding acquisition:** Allen L. Husker, Zhongwen Zhan

**Investigation:** Jiuxun Yin

**Methodology:** Jiuxun Yin, Weiqiang Zhu, Yaolin Miao

**Resources:** Zack J. Spica, Masanao Shinohara, Satoshi Ide, Kimihiro Mochizuki, Allen L. Husker, Zhongwen Zhan

**Software:** Jiuxun Yin, Weiqiang Zhu

<sup>1</sup>Seismological Laboratory, Division of Geological and Planetary Sciences, California Institute of Technology, Pasadena, CA, USA, <sup>2</sup>Department of Earth and Environmental Sciences, University of Michigan, Ann Arbor, MI, USA, <sup>3</sup>Los Alamos National Laboratory, Los Alamos, NM, USA, <sup>4</sup>Earthquake Research Institute, University of Tokyo, Bunkyo-ku, Japan, <sup>5</sup>Department of Earth and Planetary Science, University of Tokyo, Bunkyo-ku, Japan

**Abstract** Distributed Acoustic Sensing (DAS) is a promising technique to improve the rapid detection and characterization of earthquakes. Previous DAS studies mainly focus on the phase information but less on the amplitude information. In this study, we compile earthquake data from two DAS arrays in California, USA, and one submarine array in Sanriku, Japan. We develop a data-driven method to obtain the first scaling relation between DAS amplitude and earthquake magnitude. Our results reveal that the earthquake amplitudes recorded by DAS in different regions follow a similar scaling relation. The scaling relation can provide a rapid earthquake magnitude estimation and effectively avoid uncertainties caused by the conversion to ground motions. Our results show that the scaling relation appears transferable to new regions with calibrations. The scaling relation highlights the great potential of DAS in earthquake source characterization and early warning.

**Plain Language Summary** Distributed Acoustic Sensing (DAS) is an emerging technique that can convert an optical fiber cable into a dense array to record seismic waves from earthquakes. The recorded seismic signals contain essential information about earthquakes. For example, DAS can record high-amplitude signals from earthquakes with large magnitudes. However, the exact setting of the optical cables (i.e., installation conditions and coupling with the surrounding medium) is often unknown, thus preventing quantitative estimations of earthquake magnitudes with DAS. In this study, we analyze earthquake data recorded by different DAS arrays and develop a data-driven method to obtain an empirical relation between the earthquake magnitude and the amplitude of DAS signals. We show that this empirical relation can accurately estimate the earthquake magnitude directly from the DAS data. Furthermore, the empirical relation we obtain from one area can also be applied to new regions with slight calibrations. Our empirical relation can significantly expand the applications of DAS in earthquake research, such as seismic hazard assessment and earthquake early warning.

## 1. Introduction

Rapid earthquake source characterization is critical to monitor earthquakes, provide Earthquake Early Warning (EEW) alerts and prompt reactions to seismic hazards. However, this is still challenging for many remote areas with insufficient seismic station coverage. For example, subduction zones, which can hold the largest earthquakes, are generally poorly instrumented due to the large expenses involved in deploying and maintaining offshore seismic instruments. In this context, Distributed Acoustic Sensing (DAS), which can utilize pre-existing telecommunication fiber-optic cables in both onshore and offshore regions, appears to be a promising complementary sensing method to fill the geographical gaps of conventional seismic networks.

DAS is an emerging technique that has great potential in seismology. It converts every few meters of an optical fiber into a single-component strainmeter (Benioff, 1935) to provide spatially coherent signals with high sensitivity. One single DAS array often consists of thousands of channels covering tens of kilometers and can serve as a dense seismic array to achieve great spatial resolution. DAS has proved to be an effective tool to refine regional seismic structure (Ajo-Franklin et al., 2019; Spica, Nishida, et al., 2020; Spica, Pertou, et al., 2020; Trainor-Guitton et al., 2019; Viens, Pertou, et al., 2022; Yang et al., 2022; Yu et al., 2019) and to detect local earthquakes (Ajo-Franklin et al., 2019; Atterholt et al., 2022; Li & Zhan, 2018; Li et al., 2021), and seismic signals from various sources (Viens, Bonilla, et al., 2022; X. Wang et al., 2020; Williams et al., 2019; Zhan

© 2023. The Authors.

This is an open access article under the terms of the [Creative Commons Attribution-NonCommercial-NoDerivs License](#), which permits use and distribution in any medium, provided the original work is properly cited, the use is non-commercial and no modifications or adaptations are made.

**Supervision:** Allen L. Husker, Zhongwen Zhan  
**Validation:** Jiuxun Yin  
**Visualization:** Jiuxun Yin  
**Writing – original draft:** Jiuxun Yin  
**Writing – review & editing:** Jiuxun Yin, Jiaxuan Li, Ettore Biondi, Zack J. Spica, Loïc Viens, Satoshi Ide, Kimihiro Mochizuki, Allen L. Husker, Zhongwen Zhan

et al., 2021). The phase information of DAS has been well-validated to be accurate in the multiple aforementioned applications. However, DAS amplitudes, which commonly represent the direct strain/strain-rate output from an interrogator unit, are rarely considered for earthquake source characterization and early-warning purposes.

The direct use of DAS amplitude information is mainly circumscribed by a few limitations, such as unknown cable coupling, single-component sensing, uncertain instrumental response, and uncommon amplitude saturation behaviors (Lindsey et al., 2020). DAS instruments record phase shifts of light traveling in the optical fiber, and the phase information is then converted into the strain along the cable direction (Fernández-Ruiz et al., 2020; Lindsey & Martin, 2021; Lindsey et al., 2017). However, the instrumental strain is not necessarily equal to the strain of the medium surrounding the cable due to different installation methods of telecommunication cables (Ajo-Franklin et al., 2019). This coupling issue commonly exists but varies with the unknown cable installation in different regions (Ajo-Franklin et al., 2019; Lindsey et al., 2020; Paitz et al., 2020; Trainor-Guitton et al., 2019). Moreover, the instrumental response of DAS is highly frequency-dependent (Lindsey et al., 2020; Paitz et al., 2020) and often hard to quantify without co-located seismometers. The frequency-dependent instrumental response can contaminate frequency components of the DAS data and may prevent robust spectral analysis. The DAS amplitude saturation is another issue and is sometimes observed for earthquakes close to DAS instruments (Viens, Bonilla, et al., 2022). DAS amplitude saturation is often presented by a flip from maximum to minimum due to the phase wrapping of the sensing laser pulse in the cable (Ajo-Franklin et al., 2022), making this behavior hard to identify and recover. All these instrumental limitations aggravate the accurate conversion of DAS amplitude to ground motions (e.g., velocity and acceleration), thus further challenging the incorporation of DAS data into many seismology applications (Farghal et al., 2022; Lindsey & Martin, 2021). There have been many attempts to convert DAS-recorded strain to ground motions (Daley et al., 2016; Lindsey et al., 2020; Lior et al., 2021; H. F. Wang et al., 2018; Yu et al., 2019). For example, H. F. Wang et al. (2018) showed a good match between DAS amplitude and strain derived from individual co-located nodal sensors. However, in the same experiment, Muir and Zhan (2022) systematically reconstructed the strain-rate wavefield with the entire nodal array and found that the DAS-recorded amplitudes are, on average, twice that of conventional sensors. In general, accurate conversion requires good knowledge of the local geology, seismic velocity structure, and instrumental information; and is still an active research direction in the DAS community.

Instead of converting DAS-strain data to ground motion measurements (i.e., velocity or acceleration), we propose a data-driven way to explore the relationship between the peak amplitude of DAS data and earthquake magnitude. This study presents the first DAS amplitude scaling relation for a rapid magnitude estimation of DAS-recorded earthquakes. Previous studies using conventional strainmeters show that the peak strain amplitude follows an empirical relation that can be used to estimate the magnitude of earthquakes (Barbour & Crowell, 2017; Barbour et al., 2021). Unlike conventional strainmeters, one DAS array can easily provide thousands of peak amplitude measurements from a single earthquake, allowing the development of robust scaling relation with fewer earthquakes.

We analyze earthquakes recorded by DAS arrays in California, USA, and Sanriku, Japan (Figure 1). Both regions are seismically active and provide us with an unprecedented opportunity to develop and validate a DAS scaling relation. We measure peak DAS amplitudes of earthquakes based on earthquake catalogs. We apply iterative regression analysis to these datasets to obtain a robust scaling relation between the peak DAS strain rate, earthquake magnitude, and hypocentral distance, calibrated by channel-specific site terms. The obtained scaling relation can be used for rapid and reliable earthquake magnitude estimation from the DAS amplitude measurements. Furthermore, we show that the DAS amplitudes in different onshore regions follow the scaling relation with similar coefficients. The scaling relation built on terrestrial DAS arrays in California can be transferred to the submarine DAS data in Japan with calibration on the site terms.

## 2. Results

### 2.1. Data

We analyze strain-rate DAS data, which removes the instrumental drifts in our strain data and is also shown to have a frequency-independent instrumental noise at low frequency  $<0.1$  Hz (Lior et al., 2023), recorded in both terrestrial and submarine environments (Figure 1a). The DAS recording parameters and configurations are shown in Table S1 in Supporting Information S1. We start with analyzing the two terrestrial DAS arrays

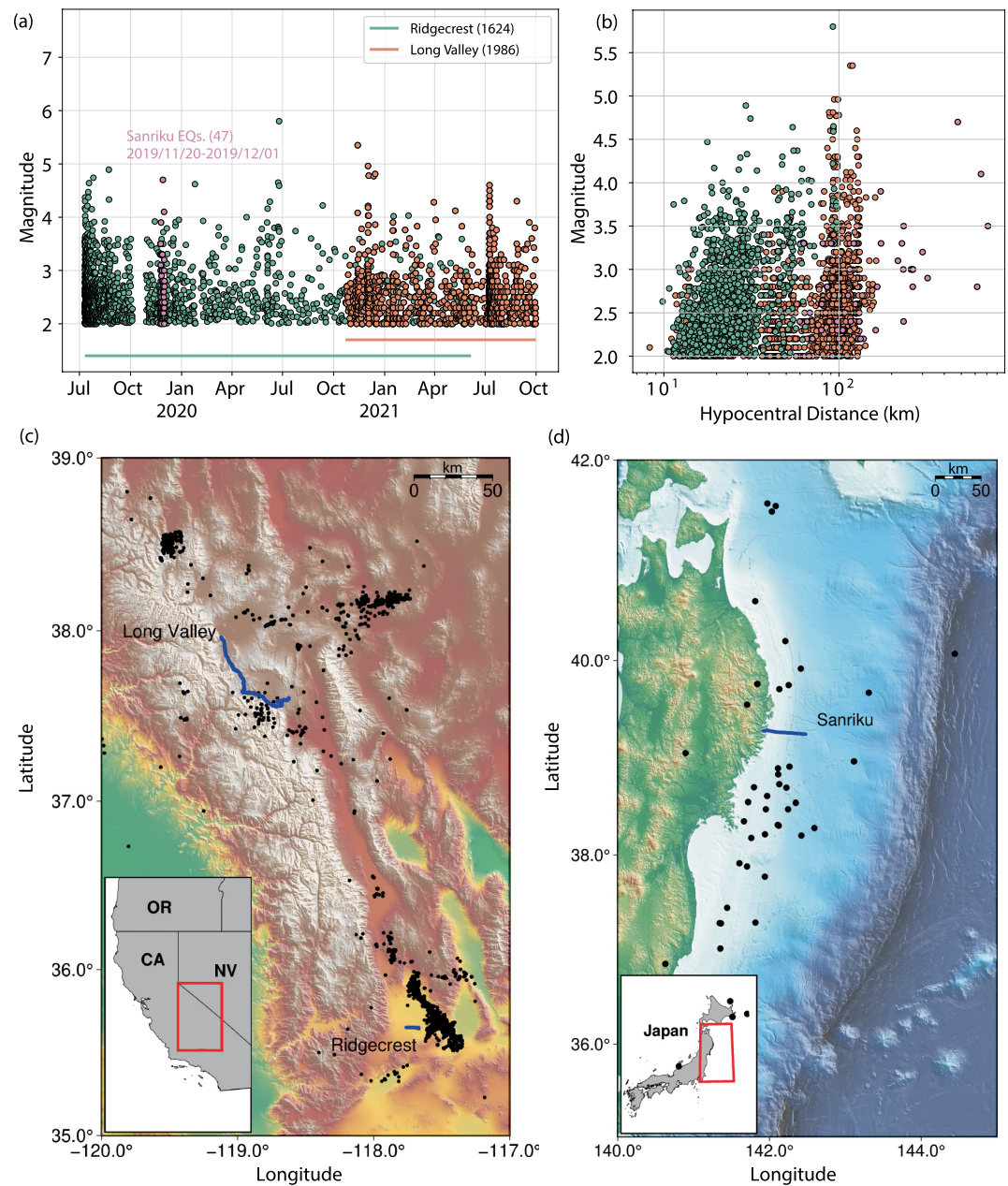


**Figure 1.** (a) Temporal distribution of earthquake magnitude from the three distributed acoustic sensing (DAS) arrays (colored circles) used in the analysis. (b) Hypocentral distance and magnitude range of earthquakes used in the analysis. The distance is the median over the array for each earthquake for better visualization. (c) Topographic map including the earthquake locations (black dots) and the Ridgecrest and Long-Valley DAS arrays (blue lines) in California, USA. (d) Map showing the locations of earthquakes (black dots) and the Sanriku DAS array (blue line) in Japan. Four earthquakes outside the main panel in (d) are shown in the inset map.

in the Ridgecrest (RC) and Long-Valley (LV) regions (Figure 1b) in California. The two arrays have recorded over 2 years of continuous data from 10 July 2019, to 31 October 2021. We first convert the DAS raw data, which is the phase shift of Rayleigh back-scattered laser signals in the optical fiber, to strain rate using Equation S1 in Supporting Information S1 (Text S1 in Supporting Information S1). We then apply PhaseNet-DAS (Zhu et al., 2023), which is a deep learning phase picker tailored for DAS data, to accurately pick P-wave and S-wave arrivals from earthquakes (Text S2 in Supporting Information S1). We associate the picked earthquakes with the regional earthquake catalogs to determine their locations and magnitudes. We also investigate 2 weeks of submarine data (from 11 November to 1 December 2019) from a DAS array in Sanriku, Japan (Shinohara et al., 2022).

The submarine DAS data suffer from various types of oceanic noise, and earthquake P-wave arrivals are rarely observed. Due to these limitations, PhaseNet-DAS is not as effective on submarine data as on terrestrial DAS arrays. Instead, we apply a template matching method to detect S-waves from earthquakes and associate them with the local Japanese Meteorological Agency (JMA) catalog for their location and magnitude (Text S3 in Supporting Information S1). In this study, we assume that the difference in catalog magnitude between the two regions, California (local magnitude  $M_L$  for most small  $M < 3$  earthquakes or moment magnitude  $M_w$  for larger  $M > 3.3$  earthquakes if available) and Sanriku  $M_{JMA}$  (velocity magnitude according to JMA (Funasaki, 2004; Katsumata, 1996)), is negligible and can be approximated as the moment magnitude to simplify the analysis (Clinton et al., 2006; Katsumata, 2004; Uhrhammer et al., 2011). This is a reasonable assumption for the earthquake magnitude range  $2 \leq M \leq 6$  analyzed in the current study, but careful analysis on different local magnitude scales is required for large  $M > 7$  earthquakes.

We successfully obtain 3,610 earthquakes with 2,363,585 P-wave and 2,411,592 S-wave peak measurements from the two California DAS arrays and 47 earthquakes with 34,803 S-wave peak measurements from the Sanriku DAS array. The California earthquakes have magnitudes ranging between M2.0 and M5.8 within hypocentral distances ranging between 5.2 and 182.6 km. The Sanriku earthquakes have magnitudes between M2.0 and M4.7 and hypocentral distances from 59.7 to 709.5 km. The measured peak DAS strain rates present strong correlations with the event magnitude (Figures 2c and 2f) and hypocentral distance (Figures 2d and 2g). Furthermore, all arrays follow similar trends, which imply the existence of a scaling relation (see Text S4 in Supporting Information S1 for details of data processing and quality control).

## 2.2. Scaling Relation

Based on the statistical correlations of data (Figure 2), we fit the data with a general form of scaling relation similar to Barbour and Crowell (2017), Barbour et al. (2021):

$$\log_{10} E_i = aM + b\log_{10} D_i + K_i, \quad (1)$$

where  $E$  is the observed peak amplitude of DAS strain rate in microstrain/s ( $10^{-6}/s$ ),  $D$  is the hypocentral distance in kilometers to each DAS channel, and  $M$  is the earthquake magnitude. The subscript  $i$  corresponds to each DAS channel. We apply an integrated channel-specific factor  $K_i$  to account for all local effects such as cable construction, installation, instrumental coupling, and the variety of regional geology.

We use an iterative regression method to fit for the magnitude coefficient  $a$ , distance coefficient  $b$ , and corresponding site terms  $K_i$  separately for P and S waves. We first apply the regression method to each individual DAS array and find that the values are almost the same among the arrays (Figure S1 in Supporting Information S1). Therefore, we combine the three California terrestrial data sets into one data set for an integrated regression. Because of the unbalanced amount of measurements and different processing steps of terrestrial and submarine DAS data, we use the California DAS data set with both P- and S-wave measurements to fit for the coefficients of Equation 1 and the Sanriku submarine DAS data as a validation set. This splitting scheme aims at testing the generality of the scaling relation. The best-fit scaling relation we obtain for P waves is:

$$\log_{10} E_i^P = 0.437M - 1.269\log_{10} D_i + K_i^P, \quad (2)$$

and for S waves is:

$$\log_{10} E_i^S = 0.690M - 1.588\log_{10} D_i + K_i^S. \quad (3)$$

We refer the reader to Text S5 and Text S6 in Supporting Information S1 for further details about the iterative regressions and site calibration terms, respectively.

## 2.3. Magnitude Estimation From DAS

We validate the scaling relation by comparing the measured peak strain rate with those calculated by the scaling relation Equation 1 to guarantee that the regression can robustly explain the features in the data (Text S7 and Figure S3 in Supporting Information S1). Then, we reorganize the scaling relation Equation 1 to estimate earthquake magnitudes from the DAS peak strain rate:

$$M_i = (\log_{10} E_i - b\log_{10} D_i - K_i) / a. \quad (4)$$



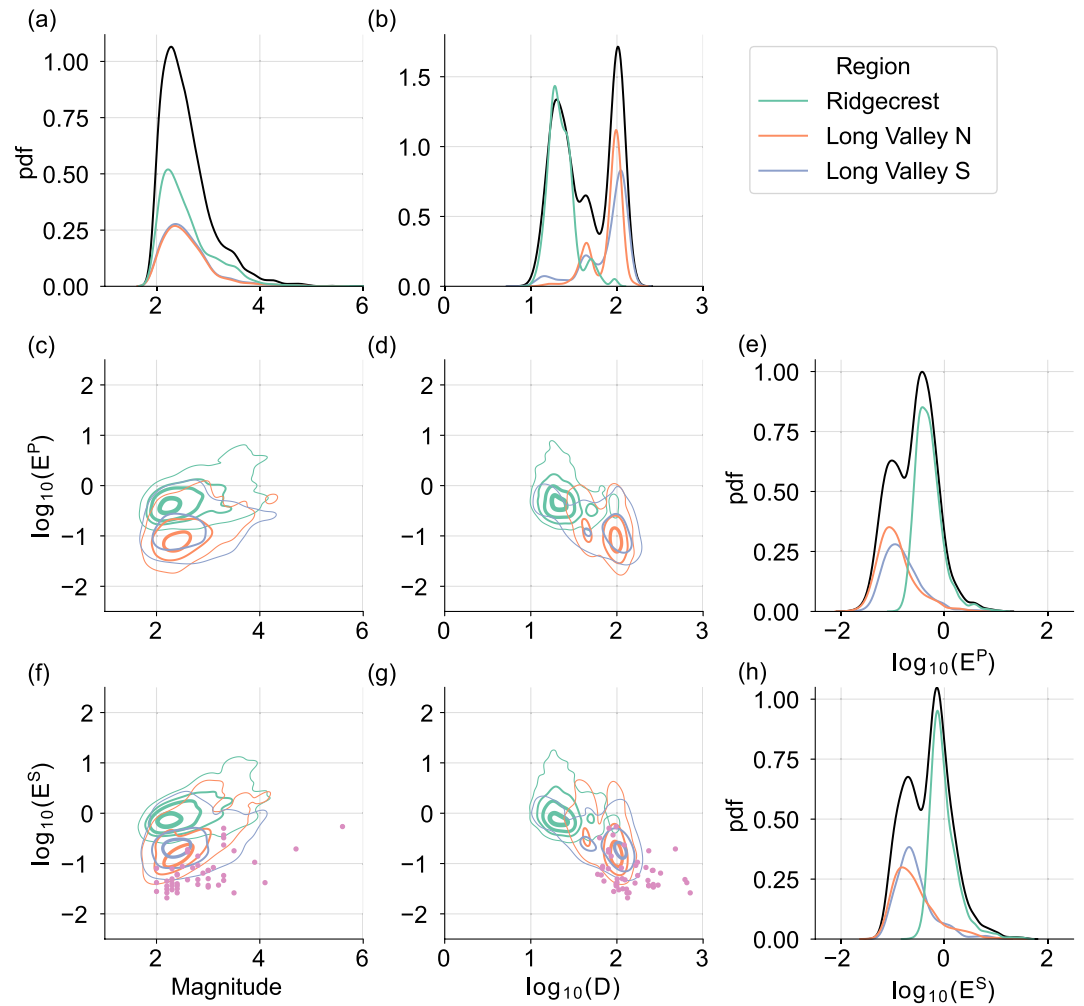


**Figure 2.** (a) Histograms in probability density function (pdf) of earthquake magnitude. (b) Histograms in pdf of hypocentral distance. (c) Magnitude versus peak P-wave distributed acoustic sensing (DAS) strain rate ( $E^P$ ). (d) Hypocentral distance versus peak P-wave DAS strain rate. (e) Histograms in pdf of peak P-wave DAS strain rate. (f) Magnitude versus peak S-wave DAS strain rate ( $E^S$ ). (g) Hypocentral distance versus peak S-wave DAS strain rate. (h) Histograms in pdf of peak S-wave DAS strain rate. For all the histograms, the black lines indicate the entire data set from all DAS arrays. Colored lines are for the individual arrays. For the 2-D correlation figures, peak DAS strain rate measurements are averaged by events. Different California arrays are shown by the colored contours, whose levels correspond to 5%, 30%, 60%, and 90% of the probability density from thin to thick lines. The Sanriku data points are shown by pink dots in (f) and (g).

Given the peak amplitude  $E_i$  and hypocentral distance  $D_i$ , we calculate the magnitude  $M_i$  for each DAS channel and then use the median magnitude of all channels as the final magnitude estimation  $M$ . Our results show that the magnitude can be reliably estimated with an error of less than 1 unit of magnitude by using either P or S waves peak amplitude in a given time window (a 2-s time window is used here, but other time windows have also been tested, see Text S4 and Table S2 in Supporting Information S1 for details) for most earthquakes in both the California and Sanriku regions, especially for the larger earthquakes (Figures 3a–3c). Moreover, we show that the scaling relation can be transferred from California to Sanriku and works equally well as that obtained from the Sanriku-only measurements (Figures 3c and 3d). The transferred scaling relation inherits the same magnitude  $a$  and hypocentral distance  $b$  coefficients from the California data set and only requires a small number of local earthquakes to recalculate the site calibration terms  $K_i$ . We apply a systematic random test to show that for the Sanriku case, only a limited number of local events (i.e., 3–6 earthquakes) are sufficient to obtain robust values of the site calibration terms (Text S8 in Supporting Information S1). The transferred scaling relation can provide a robust estimation of the magnitude of earthquakes (Figure 3d).

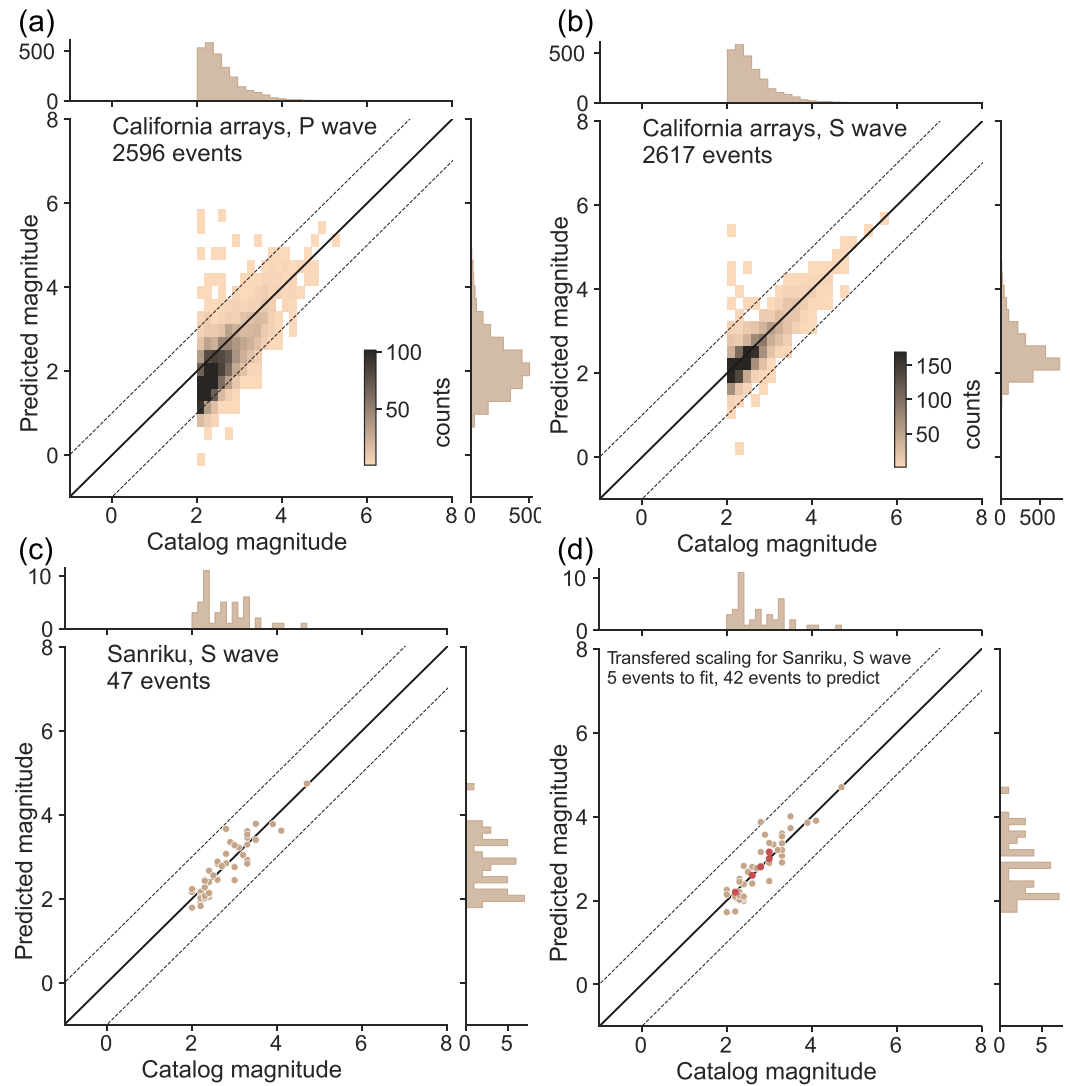


**Figure 3.** (a) P-wave scaling relation applied to the California data using all three distributed acoustic sensing (DAS) arrays. (b) S-wave scaling relation applied to California data using all three DAS arrays. (c) S-wave scaling relation applied to Sanriku data using only the Sanriku DAS array. (d) S-wave scaling relation applied to Sanriku data using scaling relation transferred from California DAS arrays. (a and b) show the 2D histograms, while (c and d) show the individual event. Red dots indicate events used for calibrating local site terms. Solid black lines show accurate estimation where catalog magnitude equals predicted magnitude, while dashed lines show plus/minus 1 unit of magnitude errors.

### 3. Discussion

#### 3.1. Transferable Scaling Relation of DAS Amplitude

Unlike conventional and well-calibrated seismic sensors, DAS instruments are commonly deployed on preexisting telecommunication optical fibers with various properties and construction designs (Ajo-Franklin et al., 2019). This generally leads to difficulties in determining the instrument responses of DAS arrays. Some previous studies have shown that DAS instrument response can be quantitatively determined by comparing DAS measurements with a co-located seismometer (Lindsey et al., 2020; Paitz et al., 2020). However, co-located sensors are not always available, especially in marine environments. There are multiple ways to convert DAS measurements to ground motions: for instance, direct calibration with co-located seismometers (Lindsey et al., 2017), correction based on apparent local phase velocity (Daley et al., 2016; Shinohara et al., 2022; H. F. Wang et al., 2018; Yu et al., 2019), spatial integration from a co-located seismometer (H. F. Wang et al., 2018), and rescaling in the  $f-k$  or curvelet domains (Lindsey et al., 2020; Yang et al., 2022). Recently, a local slant-stack transform method

was developed to convert strain to ground motion in real-time for EEW (Lior et al., 2021, 2023). Although shown to be effective, most of the conversion methods require elaborate data preprocessing and analyst-intensive quality control. Improving those methods and developing new ones are still active directions of current DAS research in the community.

This study evaluates how DAS amplitude is related to earthquake magnitude in a data-driven methodology. With the abundant peak amplitude measurements of earthquakes in the Ridgecrest and Long-Valley regions, we apply regression analysis to obtain a robust scaling relation for both P- and S-waves recorded by DAS instruments. Most importantly, we find that different regions have almost the same values of the scaling coefficients  $a$  and  $b$  (Figure S1 in Supporting Information S1). With region-specific site calibration  $K_i$  (Figures S2 and S4 in Supporting Information S1), we show that it is feasible to transfer/extrapolate the scaling relation from one well-studied area to DAS arrays in other regions for earthquakes within similar distance/magnitude ranges. The DAS peak amplitude scaling relation can be applied to earthquake source studies in different areas.

We further compare the DAS measurements with results from previous studies using conventional strainmeters (Barbour et al., 2021). The distance coefficients of both conventional strainmeters ( $b = -1.45$ ) and DAS are close, meaning that the dynamic strain follows the same geometrical spreading of wave propagation for both conventional strainmeter and DAS instruments. However, the magnitude coefficients are different ( $a = 0.92$  from strainmeters) mainly because the DAS scaling relation is obtained from strain-rate data, while the strainmeter scaling relation is based on strain data. The different physical quantities scale differently with earthquake magnitude. Strain rate is theoretically proportional to acceleration (Benioff, 1935). Therefore, we analyze the peak ground acceleration (PGA) of the Next Generation Attenuation model (NGA-West2) project (Bozorgnia et al., 2014). For consistent comparisons, we fit the PGA in the NGA-West2 data set with the same model as Equation 1, assigning the site calibration term to each station. We find that the distance coefficients from DAS ( $b = -1.27$  for the P wave and 1.59 for the S wave) are close to those from PGA ( $b = -1.63$ , Figure S1 in Supporting Information S1). The difference in the magnitude coefficients ( $a = 0.44$  for the P wave and 0.69 for the S wave from DAS vs.  $a = 0.39$  from PGA) is probably due to the different frequency bands of DAS and conventional accelerometers. Nowadays, Ground Motion Prediction Equations (GMPEs) with many parameters have been developed from various datasets to predict earthquake ground motions for engineering, and seismological applications (Boore & Atkinson, 2008; Boore et al., 2014; Bozorgnia et al., 2014; Campbell & Bozorgnia, 2014; Kanno et al., 2006; Zhao et al., 2006). Modern GMPEs have detailed definitions of distance dependence (geometrical and inelastic attenuation) and local site responses (local geology, seismic structure, instrument deployment, etc.) to explain the ground motion data in different regions. Because of the relatively early stages of the DAS technique and limited earthquake data from different locations, we only implemented the simplest form of scaling relation (i.e., Equation 1) in this study for a first-order validation of the DAS scaling relation. We leave the development of more complex DAS strain-rate prediction equations, for example, with physically defined and/or frequency-dependent site calibration terms, to future studies.

### 3.2. Potential Applications of the DAS Scaling Relation

Our peak DAS amplitude scaling relation is fundamental and significant for various seismological studies such as earthquake seismology and EEW. Regarding earthquake source analyses using DAS, the current studies mainly focus on earthquake detection and location using the time information (Atterholt et al., 2022; Lellouch et al., 2020; Li et al., 2021; Lindsey et al., 2017; Viens, Bonilla, et al., 2022; Yang et al., 2022). Adding the amplitude information and constraints on the earthquake magnitude can significantly help us resolve more source parameters and physical details about the earthquake rupture (Lior et al., 2023).

Another substantial application is for EEW, which has shown to be an effective method to mitigate seismic risk (Allen & Melgar, 2019). EEW aims to rapidly estimate ground motion from real-time data after an earthquake occurs and sends out alerts to specific users and the public. Current EEW algorithms use conventional seismic data for ground motion predictions. DAS leverages pre-existing telecommunication fiber-optic cables and can complement the current EEW systems. Converting most telecommunication cables located in highly seismic active regions into dense arrays of sensors could provide an economical approach to extending and improving the current EEW system, especially in offshore seismogenic zones.

A recent study combined DAS and GMPEs for EEW purposes (Lior et al., 2023). Their method requires conversion from DAS strain rate to ground acceleration and estimation of earthquake stress drop for earthquake

magnitude estimation. Our scaling relation provides an alternative and new approach to estimating earthquake magnitude from DAS measurements. Compared with conversion-based methods, there are advantages to using a scaling relation from direct DAS measurements. First, the scaling relation accounts for the different coupling and regional effects among DAS channels with the site calibration terms, and no manual identification of well-coupled sections of the fiber is required. Second, the scaling relation can avoid a prior estimation of stress drop: although Lior et al. (2023) have shown that the stress drop does not significantly affect the final ground motion prediction for EEW purposes, the uncertainty in stress drop estimation can bias magnitude estimation.

The scaling relation is built upon direct DAS measurements, and they do not require much pre-processing or parameter tuning, simplifying the deployment on edge-computing (Shi et al., 2016) at the instrumental sites. Furthermore, the scaling relation appears transferable to other regions, as demonstrated in the example of Sanriku data. Given a few earthquake measurements to calibrate the site terms, we can transfer the scaling relation from one well-studied region to another to apply rapid earthquake magnitude estimation.

However, this data-driven scaling analysis method also has some limitations that require further studies. The scaling relation of peak DAS amplitude relies on correct event association and peak amplitude measurement. Measurement of peak amplitude in the improper waveform window can lead to errors in the magnitude estimation. For instance, there are a few small events with largely overestimated magnitudes in our results (Figures 3a and 3b). We investigate the waveforms of those events and find that the overestimation is due to an incorrect event association. For instance, an M2 event in the Long-Valley region is estimated as an M5.5 earthquake because waveforms of this small event overlap with another large M5+ earthquake. We also find a few instances where multiple events occur in different places but are recorded at the same time, leading to overlapped arrivals in the same time window. In such cases, the peak amplitudes of weaker arrivals will be overestimated. Combining DAS with other independent seismic sensors can help to exclude the incorrectly associated event, thus improving the magnitude estimation. Amplitude saturation of DAS data (Ajo-Franklin et al., 2022; Viens, Bonilla, et al., 2022) can also affect the results and lead to under-estimated magnitude. For example, an M5.6 earthquake in the Sanriku data set has been found to be saturated (Viens, Bonilla, et al., 2022), and we had to exclude it in this study. In fact, our DAS amplitude scaling relation can help to identify whether the DAS waveform from an earthquake gets saturated if its DAS-estimated magnitude is significantly smaller than the magnitude from other methods. Finally, our current datasets only contain moderate magnitude earthquakes ( $M < 6$ ) in a few regions due to the short period of DAS deployment. Extending the similar analysis to more areas can help to further verify and improve the scaling relation. Future DAS campaigns focusing on EEW and recording large earthquakes should explore if the scaling relation still holds or behaves differently due to potential complex non-linear site response (Astorga et al., 2018; Bonilla et al., 2011; Viens, Bonilla, et al., 2022).

Finally, we conduct an idealized experiment to illustrate the potential application of the DAS scaling relation for rapid magnitude estimation. We assume that earthquakes can be immediately detected and located. Therefore, we can apply the scaling relation to the streaming earthquake signals at available DAS channels (Figures 4a and 4b) for real-time estimation of earthquake magnitude (Figures 4b and 4e). We keep the median value of magnitude estimated at each channel as the final estimation and keep updating it with time (Figures 4c and 4f). We experiment with the recent M4.57 and M5.0 earthquakes recorded by the Ridgecrest and Long-Valley north arrays. The M4.57 earthquake occurred on 15 July 2022, in the Ridgecrest region and is about 15 km from the Ridgecrest array. The M5.0 earthquake occurred on 25 October 2022, near Alum Rock and San Jose, California, and is about 244 km from the Long Valley array. Both events are not included in the data sets that are used for the regression and, therefore, are good candidates to test the scaling relation for generalization. We can reliably estimate the magnitude of both events with a magnitude uncertainty of less than 0.5 shortly after the earliest P-wave arrival. When some channels begin to detect the S wave, we also include the S wave information by averaging the magnitude from both P-wave and S-wave amplitudes to further update the magnitude estimation. Text S9 in Supporting Information S1 provides more details about the method. We also apply the same process to an M5.8 earthquake, which is the largest event in our data set recorded by the Ridgecrest array (Figure S6 in Supporting Information S1). Since this event has been used for regression, the error of magnitude estimation is less than 0.1. Lior et al. (2023) have also shown that the DAS-estimated earthquake magnitude can be combined with GMPs (Atkinson & Boore, 2006; Boore & Atkinson, 2008; Bozorgnia et al., 2014; Douglas & Edwards, 2016) to further predict the ground shaking and seismic intensity, similar to conventional EEW systems based on earthquake point source modeling (Allen & Melgar, 2019). A similar workflow also applies to the magnitude estimation from our scaling relation, and we leave that as future work.



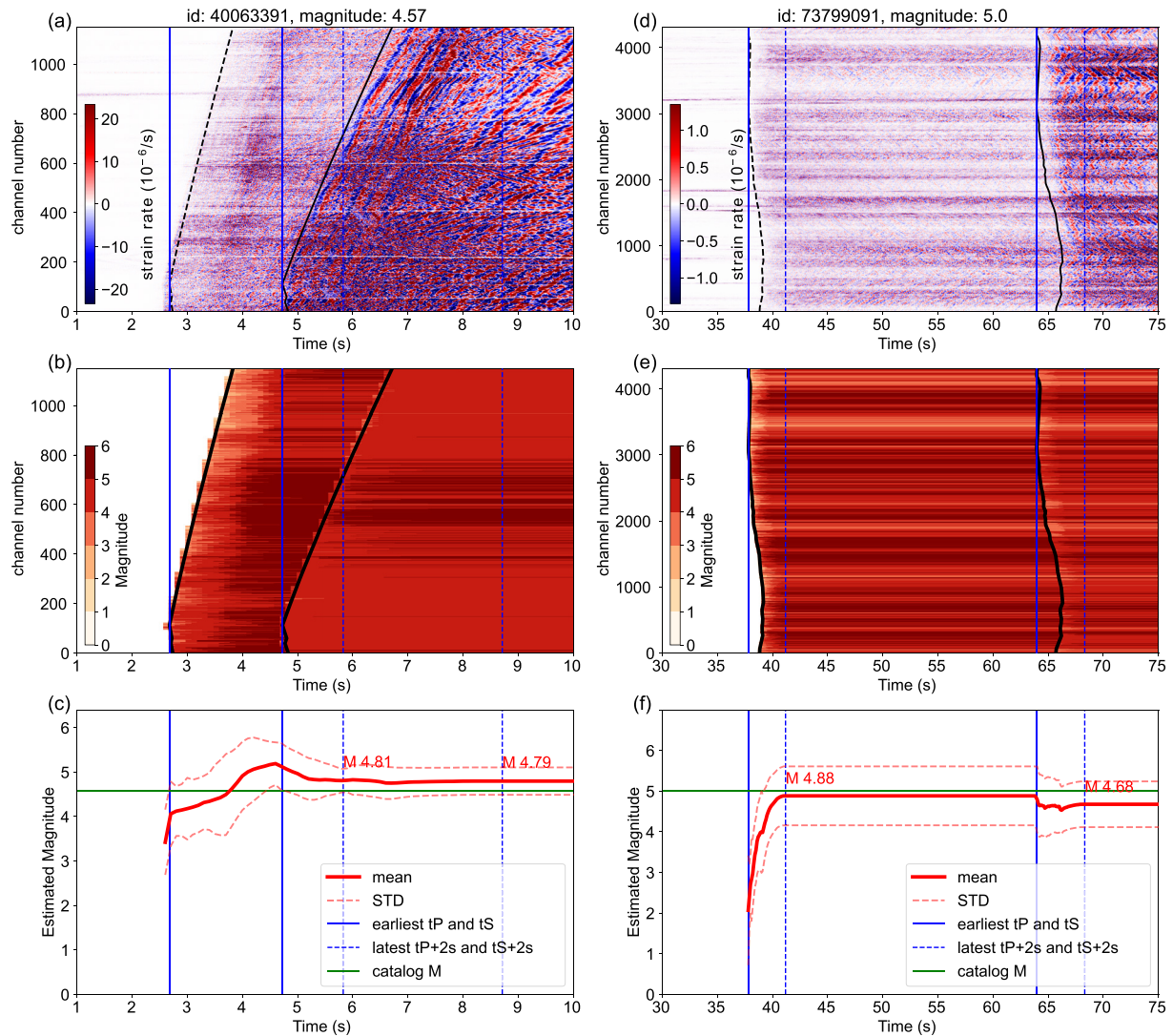


**Figure 4.** (a) Streaming distributed acoustic sensing (DAS) data from an M4.57 earthquake that occurred in the Ridgecrest region. The initial time of the earthquake is set as 0 s. (b) The corresponding magnitude estimation from the peak DAS amplitude at each channel. The black lines indicate the arrival of the P-wave and the S-wave. (c) The final magnitude estimation from averaging magnitude estimation at all available channels, shown by the red line. The red dashed lines indicate the standard deviation of magnitude estimation from channels. The green horizontal lines indicate the catalog magnitude. The blue vertical lines show the earliest P- and S- arrivals, respectively. The blue vertical dashed lines show 2 s after the latest P- and S- arrivals, respectively. (d–f) show results of another M5.0 earthquake recorded by Long Valley north array.

## 4. Conclusion

This work presents the first scaling relation between DAS peak amplitude, earthquake magnitude, and hypocentral distance from terrestrial and submarine DAS arrays. We show that the scaling relation can be used to rapidly estimate the magnitude of earthquakes. Furthermore, we find that the scaling relation appears transferable from terrestrial DAS arrays in California to a submarine DAS array in Sanriku, Japan, with minor calibrations. The DAS amplitude scaling relation has great potential in different seismological studies, such as EEW and earthquake source characterization.

## Data Availability Statement

The measured peak strain rate amplitude from multiple DAS arrays is available from the Caltech DATA repository <https://data.caltech.edu/records/sk6em-th949> with <https://doi.org/10.22002/sk6em-th949>. The Python scripts to process the data and reproduce results are available at <https://github.com/yinjiuxun/das-strain-scaling>.

### Acknowledgments

The authors would like to thank Jessie Saunders and Egill Hauksson at the California Institute of Technology and Richard Allen at the University of California, Berkeley, for their helpful suggestions. The authors also appreciate the constructive comments, which greatly improved the manuscript, from Itzhak Lior and the other anonymous reviewer. This work was supported by the Office of Emergency Services, State of California, under MCG.CEEWS3-1-CALIFOES. NEWS, funding source award number 6113-2019. Y.M. is supported by NSF award EAR2022716. L.V. is supported by the Chick Keller Fellowship from the Center for Space and Earth Science (CSES) at Los Alamos National Laboratory (LANL). CSES is funded by LANL's Laboratory Directed Research and Development (LDRD) program under project number 20210528CR. This article has a Los Alamos National Laboratory (LANL) Unlimited Release Number (LA-UR-23-20408).

### References

- Ajo-Franklin, J., Rodríguez Tribaldos, V., Nayak, A., Cheng, F., Mellors, R., Chi, B., et al. (2022). The imperial valley dark fiber project: Toward seismic studies using das and telecom infrastructure for geothermal applications. *Seismological Research Letters*, 93(5), 2906–2919. <https://doi.org/10.1785/0220220072>
- Ajo-Franklin, J. B., Dou, S., Lindsey, N. J., Monga, I., Tracy, C., Robertson, M., et al. (2019). Distributed acoustic sensing using dark fiber for near-surface characterization and broadband seismic event detection. *Scientific Reports*, 9(1), 1328. <https://doi.org/10.1038/s41598-018-36675-8>
- Allen, R. M., & Melgar, D. (2019). Earthquake early warning: Advances, scientific challenges, and societal needs. *Annual Review of Earth and Planetary Sciences*, 47(1), 361–388. <https://doi.org/10.1146/annurev-earth-053018-060457>
- Astorga, A., Guéguen, P., & Kashima, T. (2018). Nonlinear elasticity observed in buildings during a long sequence of earthquakes. *Bulletin of the Seismological Society of America*, 108(3A), 1185–1198. <https://doi.org/10.1785/0120170289>
- Atkinson, G. M., & Boore, D. M. (2006). Earthquake ground-motion prediction equations for eastern North America. *Bulletin of the Seismological Society of America*, 96(6), 2181–2205. <https://doi.org/10.1785/0120050245>
- Atterholt, J., Zhan, Z., Shen, Z., & Li, Z. (2022). A unified wavefield-partitioning approach for distributed acoustic sensing. *Geophysical Journal International*, 228(2), 1410–1418. <https://doi.org/10.1093/gji/ggab407>
- Barbour, A. J., & Crowell, B. W. (2017). Dynamic strains for earthquake source characterization. *Seismological Research Letters*, 88(2), 354–370. <https://doi.org/10.1785/0220160155>
- Barbour, A. J., Langbein, J. O., & Farghal, N. S. (2021). Earthquake magnitudes from dynamic strain. *Bulletin of the Seismological Society of America*, 111(3), 1325–1346. <https://doi.org/10.1785/0120200360>
- Benioff, H. (1935). A linear strain seismograph. *Bulletin of the Seismological Society of America*, 25(4), 283–309. <https://doi.org/10.1785/bssa0250040283>
- Bonilla, L. F., Tsuda, K., Pulido, N., Régnier, J., & Laurendeau, A. (2011). Nonlinear site response evidence of K-NET and KiK-net records from the 2011 off the Pacific coast of Tohoku earthquake. *Earth Planets and Space*, 63(7), 785–789. <https://doi.org/10.5047/eps.2011.06.012>
- Boore, D. M., & Atkinson, G. M. (2008). Ground-motion prediction equations for the average horizontal component of PGA, PGV, and 5 periods between 0.01 s and 10.0 s. *Earthquake Spectra*, 24(1), 99–138. <https://doi.org/10.1193/1.2830434>
- Boore, D. M., Stewart, J. P., Seyhan, E., & Atkinson, G. M. (2014). NGA-West2 equations for predicting PGA, PGV, and 5 earthquakes. *Earthquake Spectra*, 30(3), 1057–1085. <https://doi.org/10.1193/070113EQS184M>
- Bozorgnia, Y., Abrahamson, N. A., Atik, L. A., Anchet, T. D., Atkinson, G. M., Baker, J. W., et al. (2014). NGA-West2 research project. *Earthquake Spectra*, 30(3), 973–987. <https://doi.org/10.1193/072113EQS209M>
- Campbell, K. W., & Bozorgnia, Y. (2014). NGA-West2 ground motion model for the average horizontal components of PGA, PGV, and 5% damped linear acceleration response spectra. *Earthquake Spectra*, 30(3), 1087–1115. <https://doi.org/10.1193/062913EQS175M>
- Clinton, J. F., Hauksson, E., & Solanki, K. (2006). An evaluation of the SCSN moment tensor solutions: Robustness of the  $M_w$  magnitude scale, style of faulting, and automation of the method. *Bulletin of the Seismological Society of America*, 96(5), 1689–1705. <https://doi.org/10.1785/0120050241>
- Daley, T. M., Miller, D. E., Dodds, K., Cook, P., & Freifeld, B. M. (2016). Field testing of modular borehole monitoring with simultaneous distributed acoustic sensing and geophone vertical seismic profiles at citronelle, Alabama. *Geophysical Prospecting*, 64(5), 1318–1334. <https://doi.org/10.1111/1365-2478.12324>
- Douglas, J., & Edwards, B. (2016). Recent and future developments in earthquake ground motion estimation. *Earth-Science Reviews*, 160, 203–219. <https://doi.org/10.1016/j.earscirev.2016.07.005>
- Farghal, N. S., Saunders, J. K., & Parker, G. A. (2022). The potential of using fiber optic distributed acoustic sensing (DAS) in earthquake early warning applications. *Bulletin of the Seismological Society of America*, 12(3), 1416–1435. <https://doi.org/10.1785/0120210214>
- Fernández-Ruiz, M. R., Soto, M. A., Williams, E. F., Martín-Lopez, S., Zhan, Z., Gonzalez-Herrera, M., & Martins, H. F. (2020). Distributed acoustic sensing for seismic activity monitoring. *APL Photonics*, 5(3), 030901. <https://doi.org/10.1063/1.5139602>
- Funasaki, J. (2004). Revision of the JMA velocity magnitude. *Quarterly Journal of Seismology*, 67, 11–20.
- Kanno, T., Narita, A., Morikawa, N., Fujiwara, H., & Fukushima, Y. (2006). A new attenuation relation for strong ground motion in Japan based on recorded data. *Bulletin of the Seismological Society of America*, 96(3), 879–897. <https://doi.org/10.1785/0120050138>
- Katsumata, A. (1996). Comparison of magnitudes estimated by the Japan Meteorological Agency with moment magnitudes for intermediate and deep earthquakes. *Bulletin of the Seismological Society of America*, 86(3), 832–842. <https://doi.org/10.1785/bssa0860030832>
- Katsumata, A. (2004). Revision of the JMA displacement magnitude. *Quarterly Journal of Seismology*, 67, 1–10.
- Lellouch, A., Lindsey, N. J., Ellsworth, W. L., & Biondi, B. L. (2020). Comparison between distributed acoustic sensing and geophones: Downhole microseismic monitoring of the forge geothermal experiment. *Seismological Research Letters*, 91(6), 3256–3268. <https://doi.org/10.1785/0220200149>
- Li, Z., Shen, Z., Yang, Y., Williams, E., Wang, X., & Zhan, Z. (2021). Rapid response to the 2019 Ridgecrest earthquake with distributed acoustic sensing. *AGU Advances*, 2(2), e2021AV000395. <https://doi.org/10.1029/2021AV000395>
- Li, Z., & Zhan, Z. (2018). Pushing the limit of earthquake detection with distributed acoustic sensing and template matching: A case study at the brady geothermal field. *Geophysical Journal International*, 215(3), 1583–1593. <https://doi.org/10.1093/gji/ggy359>
- Lindsey, N. J., & Martin, E. R. (2021). Fiber-optic seismology. *Annual Review of Earth and Planetary Sciences*, 49(1), 309–336. <https://doi.org/10.1146/annurev-earth-072420-065213>
- Lindsey, N. J., Martin, E. R., Dreger, D. S., Freifeld, B., Cole, S., James, S. R., et al. (2017). Fiber-optic network observations of earthquake wavefields. *Geophysical Research Letters*, 44(23), 11792–11799. <https://doi.org/10.1002/2017GL075722>
- Lindsey, N. J., Rademacher, H., & Ajo-Franklin, J. B. (2020). On the broadband instrument response of fiber-optic das arrays. *Journal of Geophysical Research: Solid Earth*, 125(2), e2019JB018145. <https://doi.org/10.1029/2019JB018145>
- Lior, I., Rivet, D., Ampuero, J.-P., Sladen, A., Barrientos, S., Sánchez-Olivarría, R., et al. (2023). Magnitude estimation and ground motion prediction to harness fiber optic distributed acoustic sensing for earthquake early warning. *Scientific Reports*, 13(1), 424. <https://doi.org/10.1038/s41598-023-27444-3>
- Lior, I., Sladen, A., Mercerat, D., Ampuero, J.-P., Rivet, D., & Sambolian, S. (2021). Strain to ground motion conversion of distributed acoustic sensing data for earthquake magnitude and stress drop determination. *Solid Earth*, 12(6), 1421–1442. <https://doi.org/10.5194/se-12-1421-2021>
- Muir, J. B., & Zhan, Z. (2022). Wavefield-based evaluation of DAS instrument response and array design. *Geophysical Journal International*, 229(1), 21–34. <https://doi.org/10.1093/gji/ggab439>
- Paiz, P., Edme, P., Gräff, D., Walter, F., Doetsch, J., Chalari, A., et al. (2020). Empirical investigations of the instrument response for distributed acoustic sensing (DAS) across 17 Octaves. *Bulletin of the Seismological Society of America*, 111(1), 1–10. <https://doi.org/10.1785/0120200185>

- Shi, W., Cao, J., Zhang, Q., Li, Y., & Xu, L. (2016). Edge computing: Vision and challenges. *IEEE Internet of Things Journal*, 3(5), 637–646. <https://doi.org/10.1109/jiot.2016.2579198>
- Shinohara, M., Yamada, T., Akuhara, T., Mochizuki, K., & Sakai, S. (2022). Performance of seismic observation by distributed acoustic sensing technology using a seafloor cable off Sanriku, Japan. *Frontiers in Marine Science*, 9, 466. <https://doi.org/10.3389/fmars.2022.844506>
- Spica, Z. J., Nishida, K., Akuhara, T., Pétrélis, F., Shinohara, M., & Yamada, T. (2020a). Marine sediment characterized by ocean-bottom fiber-optic seismology. *Geophysical Research Letters*, 47(16), e2020GL088360. <https://doi.org/10.1029/2020GL088360>
- Spica, Z. J., Pertont, M., Martin, E. R., Beroza, G. C., & Biondi, B. (2020b). Urban seismic site characterization by fiber-optic seismology. *Journal of Geophysical Research: Solid Earth*, 125(3), e2019JB018656. <https://doi.org/10.1029/2019JB018656>
- Trainor-Guitton, W., Guitton, A., Jreij, S., Powers, H., & Sullivan, B. (2019). 3D imaging of geothermal faults from a vertical das fiber at Brady Hot Spring, NV USA. *Energies*, 12(7), 1401. <https://doi.org/10.3390/en12071401>
- Uhrhammer, R., Hellweg, M., Hutton, K., Lombard, P., Walters, A., Hauksson, E., & Oppenheimer, D. (2011). California integrated seismic network (CISN) local magnitude determination in California and vicinity. *Bulletin of the Seismological Society of America*, 101(6), 2685–2693. <https://doi.org/10.1785/0120100106>
- Viens, L., Bonilla, L. F., Spica, Z. J., Nishida, K., Yamada, T., & Shinohara, M. (2022a). Nonlinear earthquake response of marine sediments with distributed acoustic sensing. *Geophysical Research Letters*, 49(21), e2022GL100122. <https://doi.org/10.1029/2022GL100122>
- Viens, L., Pertont, M., Spica, Z. J., Nishida, K., Shinohara, M., & Yamada, T. (2022b). Understanding surface-wave modal content for high-resolution imaging of submarine sediments with distributed acoustic sensing.
- Wang, H. F., Zeng, X., Miller, D. E., Fratta, D., Feigl, K. L., Thurber, C. H., & Mellors, R. J. (2018). Ground motion response to an ml 4.3 earthquake using co-located distributed acoustic sensing and seismometer arrays. *Geophysical Journal International*, 213(3), 2020–2036. <https://doi.org/10.1093/gji/ggy102>
- Wang, X., Williams, E. F., Karrenbach, M., Herráez, M. G., Martins, H. F., & Zhan, Z. (2020). Rose parade seismology: Signatures of floats and bands on optical fiber. *Seismological Research Letters*, 91(4), 2395–2398. <https://doi.org/10.1785/0220200091>
- Williams, E. F., Fernández-Ruiz, M. R., Magalhaes, R., Vanthillo, R., Zhan, Z., González-Herráez, M., & Martins, H. F. (2019). Distributed sensing of microseisms and teleseisms with submarine dark fibers. *Nature Communications*, 10(1), 5778. <https://doi.org/10.1038/s41467-019-13262-7>
- Yang, Y., Atterholt, J. W., Shen, Z., Muir, J. B., Williams, E. F., & Zhan, Z. (2022). Sub-kilometer correlation between near-surface structure and ground motion measured with distributed acoustic sensing. *Geophysical Research Letters*, 49(1), e2021GL096503. <https://doi.org/10.1029/2021GL096503>
- Yu, C., Zhan, Z., Lindsey, N. J., Ajo-Franklin, J. B., & Robertson, M. (2019). The potential of das in teleseismic studies: Insights from the goldstone experiment. *Geophysical Research Letters*, 46(3), 1320–1328. <https://doi.org/10.1029/2018GL081195>
- Zhan, Z., Cantono, M., Kamalov, V., Mecozzi, A., Müller, R., Yin, S., & Castellanos, J. C. (2021). Optical polarization-based seismic and water wave sensing on transoceanic cables. *Science*, 371(6532), 931–936. <https://doi.org/10.1126/science.abe6648>
- Zhao, J. X., Zhang, J., Asano, A., Ohno, Y., Oouchi, T., Takahashi, T., & Fukushima, Y. (2006). Attenuation relations of strong ground motion in Japan using site classification based on predominant period. *Bulletin of the Seismological Society of America*, 96(3), 898–913. <https://doi.org/10.1785/0120050122>
- Zhu, W., Biondi, E., Li, J., Yin, J., Ross, Z. E., & Zhan, Z. (2023). Seismic arrival-time picking on distributed acoustic sensing data using semi-supervised learning. arXiv preprint.

## References From the Supporting Information

- Aoi, S., Asano, Y., Kunugi, T., Kimura, T., Uehira, K., Takahashi, N., et al. (2020). MOWLAS: NIED observation network for earthquake, tsunami and volcano. *Earth Planets and Space*, 72(1), 126. <https://doi.org/10.1186/s40623-020-01250-x>
- Dziewonski, A. M., Chou, T.-A., & Woodhouse, J. H. (1981). Determination of earthquake source parameters from waveform data for studies of global and regional seismicity. *Journal of Geophysical Research*, 86(B4), 2825–2852. <https://doi.org/10.1029/JB086iB04p02825>
- Shelly, D. R., Beroza, G. C., & Ide, S. (2007). Non-volcanic tremor and low-frequency earthquake swarms. *Nature*, 446(7133), 305–307. <https://doi.org/10.1038/nature05666>
- Zhu, W., & Beroza, G. C. (2019). PhaseNet: A deep-neural-network-based seismic arrival-time picking method. *Geophysical Journal International*, 216(1), 261–273.